

Measurement of the Electron Affinity of Cerium

V. T. Davis

Department of Physics, United States Military Academy, West Point, New York 10996

J. S. Thompson

Department of Physics and Chemical Physics Program, University of Nevada, Reno, Nevada 89557-0058

(Received 28 August 2001; published 5 February 2002)

The electron affinity of cerium has been measured using laser photodetachment electron spectroscopy. The electron affinity of $\text{Ce}(\text{}^1\text{G}_4)$ was determined to be 0.955 ± 0.026 eV. The data also show that Ce^- has at least two bound excited states with binding energies of 0.921 ± 0.025 eV and 0.819 ± 0.027 eV relative to the $(\text{}^1\text{G}_4)$ ground state of the cerium atom. The present experimental measurements are compared to recent calculations of the energy levels of Ce^- . Strong disagreement with the most recent theoretical atomic structure calculations highlights the complicated nature of this particular lanthanide.

DOI: 10.1103/PhysRevLett.88.073003

PACS numbers: 32.10.Hq, 32.80.Gc

Studies of negative ions have resulted in advances in the understanding of electron-electron interactions in many-bodied calculations designed to model the properties of atoms, molecules, and clusters. For example, accurate calculations of the binding energy of the extra electron, for even simple anionic atomic systems, requires sophisticated calculations that include a detailed accounting of effects that can be ignored in many atomic structure calculations. Several recent reviews of negative ion research [1–3] have pointed out the computational complexity encountered by theoretical investigations of lanthanide negative ions and the paucity of experimentally derived information for these ions. The importance of experimentally determined parameters, such as electron affinities (EA), is crucial to the understanding of the electron-electron interactions which are responsible for the existence of negative ions.

Negative ion structure calculations are difficult, and approximations are typically used in the calculations to reduce the number of terms contributing to the energy levels, so as to make the calculations tractable. Furthermore, as atomic Z increases, the relative contributions of electron correlation and relativistic effects become comparable, increasing the complexity of the calculation. The lanthanides are particularly interesting physically because of their unique properties, which result from the relationship of their $4f$, $5d$, and $6s$ electrons to one another. Although the small radii of the $4f$ orbitals shield them from outside influences, their binding energies are nevertheless comparable to their outer neighbors. Since the spread of energies within a particular configuration is much larger than the spread in those binding energies, the various configurations overlap one another to a considerable degree, making theoretical calculations based on the mixing of configurational basis functions extremely difficult [4]. This is particularly true in the case of cerium, which, except for Gd, is the only lanthanide with two partially filled subshells ($4f$ and $5d$). Experimental verification of the existence of the predicted negative ion structure is therefore

necessary to judge the validity of theoretical approximations. In particular, since knowledge of the electron affinities of rare-earth atoms is limited, there is keen interest in experimental data concerning the electron affinities of the lanthanides [1].

Semiempirical estimates of the electron affinities of certain lanthanides have been made in the past [5–7]. A more recent theoretical calculation by O'Malley and Beck [8] was based on a relativistic configuration interaction calculation method which begins with a zeroth-order multiconfigurational Dirac-Fock solution. This calculation yielded an electron affinity of cerium as 0.428 eV with a ground-state configuration for Ce^- of $[\text{Xe}](4f5d^36s)$ and a prediction of 14 excited states of Ce^- , six of which belong to the ground-state configuration, and the other eight with a configuration $[\text{Xe}](4f5d6s^26p)$ [8]. The difficult nature of these calculations for Ce is highlighted by the fact that these calculations are refinements of a previous calculation by the same method, in which the electron affinity (EA) of Ce was reported to be 0.259 eV [9]. Improvements in the calculations were reportedly due to a better treatment of second order effects and a more suitable choice of a neutral threshold [8].

Previous experimental investigators have reported production of stable lanthanide negative ions (to include cerium) using accelerator mass spectrometry (AMS) techniques [10,11]. The reported negative ion production yields for La^- and Ce^- were much higher than for the other atomic lanthanides, indicating that either the electron affinities of lanthanum and cerium are greater than other rare-earth atoms or La^- and Ce^- have more than one bound state [10,11]. The theoretical predictions of O'Malley and Beck [8] bear this out. Also, subsequent experimental studies have confirmed the existence of an excited bound state for La^- [12]. Nadeau *et al.* have reported measurements of the electron affinities of Tm, Yb, and Dy using an electric field dissociation technique [13], although some of these results are disputed [14]. The relative yields of sputtered negative ions can be used

to compare binding energies, but only as an indication of relative values. Using this technique, Nadeau *et al.* have reported a lower limit of 0.5 eV for the binding energy of Ce^- [11]. Berkovits *et al.*, using a combination of laser excitation and AMS, reported an EA for Ce of 0.7 eV [15]. This admittedly tentative result was based, in part, on the unrefined calculations of Dinov *et al.* [9] and the energy separation of two unidentified photodetachment threshold channels. Also of importance is a recent laser photodetachment electron spectroscopy (LPES) experimental determination of the EA of Lu [16].

This experimental study of Ce^- was performed using the LPES technique. A detailed description of the experimental apparatus has been given elsewhere [17], so only a brief description is presented. The experimental apparatus consisted of a commercial cesium-sputter negative-ion source, an accelerator, and an interaction chamber in which photoelectrons were produced and analyzed. The source of the negative ions was a target pellet consisting of a mixture of copper powder, cerium powder, sodium carbonate, and cerium iron oxide. The negative ions produced were accelerated by a 10 kV potential, mass selected by a 90° bending magnet, then focused and steered into the interaction chamber. Once inside the chamber, the ion beam intersected a photon beam at an intersection angle of 90° . Two lasers were used to produce photons for this experiment: an argon-ion laser operating in a single-line mode at a wavelength of 514.5 nm and typically delivering 1–2 W to the interaction chamber, and a continuous Nd:YAG laser operating in a single-line mode at 1064 nm and typically delivering between 6–8 W to the interaction chamber.

Electrons photodetached in the interaction region were energy analyzed using a spherical-sector, 160° electrostatic kinetic energy analyzer which operated in a fixed pass-energy mode. The electron spectrometer was positioned below the plane which contained the laser and ion beams. For all the measurements presented in this Letter, the spectrometer was located at a 45° declination angle. Electrons with the correct energy for transmission through the spherical-sector analyzer were detected with a channel electron multiplier. Analog outputs from the ion beam current and the laser power meters were converted to frequencies by a voltage-to-frequency converter and logged with counters for normalization of electron counts.

A typical photoelectron kinetic energy spectrum for Ce^- taken with the argon-ion laser is shown in Fig. 1. Copper dimer anions ($^A\text{Cu}_2^-$, $A = 126, 130$) produced from sputtering of the copper powder were used as mass markers to identify the $^{140}\text{Ce}^-$ beam. Thirty-five Ce^- photoelectron spectra were recorded using the argon-ion laser. The energy scale for all the Ce^- photoelectron kinetic energy spectra taken with the argon-ion laser was determined using the photoelectron energy spectra of Cu^- and the known EA of Cu [18]. Electron energy spectra

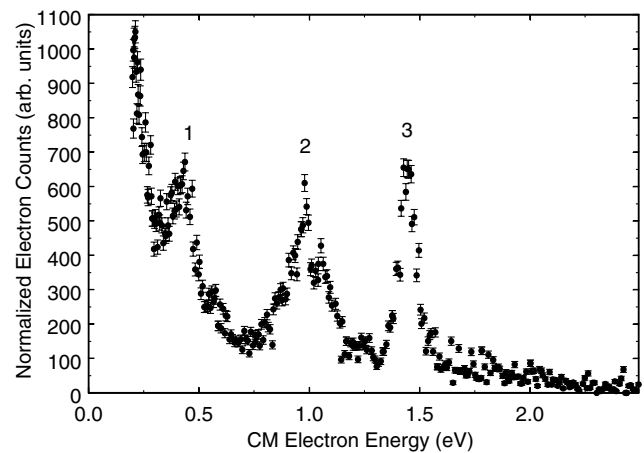


FIG. 1. Typical photoelectron kinetic energy spectrum for photodetaching Ce^- using an argon-ion laser (514.5 nm). The laser output power was 1.4 W. The kinetic energy of the Ce^- ions in the beam was 10 keV, and the ion current, measured in the interaction chamber, was 500 pA. The data accumulation time for each data point was 120 sec and the spectrum took approximately 4 h to complete.

were taken for the photodetachment of Cu^- before or after each Ce^- photoelectron spectrum was accumulated.

The energy scale for the Ce^- photoelectron spectra in the laboratory frame was then transformed into the ion rest frame using the Cu^- photoelectron spectra as a reference. The spectra were then interpreted using spectroscopic data for the cerium atom [19]. The energy separation of the photoelectron peaks correspond to the initial and final states for the process $h\nu + \text{Ce}^- \rightarrow \text{Ce} + e^-$, where Ce and Ce^- can be in excited states. Conservation of energy requires that the kinetic energy of the photoelectron, E_c , is given by

$$E_c = E_\gamma - E_e^a - E_a + E_e^n, \quad (1)$$

where E_γ is the photon energy, E_e^a is the excitation energy of the final state of the atom, E_a is the electron affinity, and E_e^n is the excitation energy of the initial negative ion state.

The photoelectron peaks in Fig. 1 were fit to Gaussian functions using a weighted least-squares technique to determine the energy centroid of each peak. The width of each Gaussian peak was fixed to match the width of each fine-structure resolved Cu^- reference scan. Decomposition of peak 2 reveals at least four transitions of energies 1.326 ± 0.038 eV, 1.408 ± 0.045 eV, 1.477 ± 0.048 eV, and 1.572 ± 0.054 eV. Peak 1 reveals at least two, and possibly three additional transitions were also observed in the 2 eV range (2.020 ± 0.042 eV, 2.089 ± 0.042 eV, 2.168 ± 0.029 eV). The observed increase in electron counts near 0 eV was due to low energy electrons created by collisional detachment of Ce^- ions in the beam by background gas and ion-aperture scattering.

An examination of Fig. 1 also shows that the structure labeled 3 is the most intense feature, and since there are no discernible higher energy structures, we conclude that the information about the ground-state to ground-state transition is contained therein. Therefore, to determine the EA of cerium, the transitions contained in that feature were studied in more detail, using a Nd:YAG laser, which was capable of producing a greater photon flux.

A typical photoelectron kinetic energy spectrum for Ce^- taken with the Nd:YAG laser is shown in Fig. 2. Thirteen Ce^- photoelectron spectra were recorded using the Nd:YAG laser. The energy scale for all the Ce^- photoelectron kinetic energy spectra taken with the Nd:YAG laser was determined using the photoelectron energy spectra of Na^- produced by the sputtering of the sodium carbonate and the known EA of Na [1]. Electron energy spectra were taken for the photodetachment of Na^- either before or after each Ce^- photoelectron spectrum was accumulated. The energy scale for the Ce^- photoelectron spectra in the laboratory frame was then referenced to the Na^- photoelectron spectra and fit using the least-squares technique as described above.

An investigation of the width of the structure shown in Fig. 2 indicated that it was composed of photoelectrons from more than one photodetachment channel (the width of each Gaussian peak was fixed to match the width of each fine-structure resolved Na^- reference scan). Decomposition of the peak 3 structure shows at least six transitions, the strongest of which represents the actual EA of cerium. Diagram A is an energy level diagram of the experimentally determined weighted averages of the photoelectron

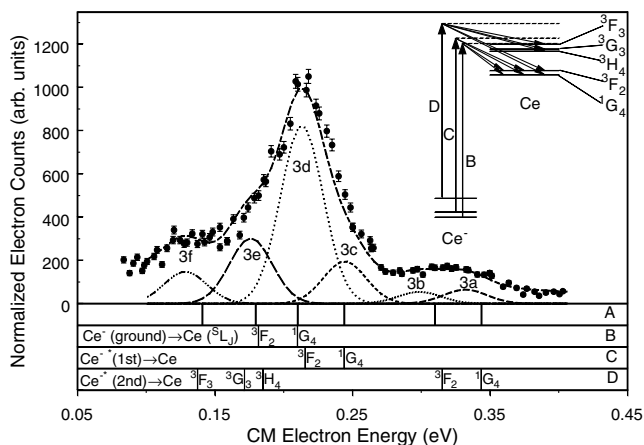


FIG. 2. Typical photoelectron kinetic energy spectrum for photodetaching Ce^- using a Nd:YAG laser (1064 nm). The laser output power was 6.70 W. The kinetic energy of the Ce^- ions in the beam for this spectrum was 10 keV, and the ion current, measured in the interaction chamber, was approximately 300 pA. The data accumulation time for each data point was 90 sec and the spectrum took approximately 3.75 h to complete. The inset in the upper right is a schematic of the energy level diagrams for Ce and Ce^- . The peaks in the spectra are labeled for further identification in the text. The energy level diagrams (labeled A, B, C, and D) are discussed in the text.

energies associated with peaks 3a–3f. The spacing of the energies in this diagram was crucial to the interpretation of the data in this experiment. The diagram labeled B in Fig. 2 is an energy level diagram of the first two states of neutral Ce: ($^1\text{G}_4$) and ($^3\text{F}_2$) [19]. Overlaying this diagram to the spectrum and diagram A shows that the peaks in Fig. 2 labeled 3d and 3e represent transitions from the ground state of the negative ion to the ground state and first excited state of neutral Ce, respectively. The diagram labeled C in Fig. 2 is also an energy level diagram of the first two states of neutral Ce but is shifted from diagram B by the experimentally measured difference between the binding energies of the ground state and first excited state of Ce^- . Overlaying this diagram onto the figure shows that the peak labeled 3c represents a transition from the first excited state of the negative ion to the ground state of the neutral. It also indicates that peak 3d, in addition to containing the information described above, also contains the information from the Ce^- (first excited state) \rightarrow $\text{Ce}(^3\text{F}_2)$ transition. The diagram labeled D in Fig. 2 is an energy level diagram of the first five states of neutral Ce and is shifted from diagram C by the experimentally measured difference between the binding energies of the first two excited states of Ce^- . Overlaying this diagram onto the figure shows that the peaks labeled 3a and 3b represent transitions from the second excited state of the negative ion to the ground state and first excited state of neutral Ce, respectively. The peak labeled 3f represents the transition Ce^- (second excited state) \rightarrow $\text{Ce}(^3\text{F}_3)$. Figure 2 also indicates that peak 3e, in addition to containing the information described above, also contains the information from the transitions Ce^- (second excited state) \rightarrow $\text{Ce}(^3\text{H}_4)$, and Ce^- (second excited state) \rightarrow $\text{Ce}(^3\text{G}_3)$. The energy level diagrams (B, C, and D) and the experimentally determined photoelectron energies (diagram A) are in excellent agreement and support the interpretation of the data presented above.

The photopeaks 3a, 3c, and 3d in Fig. 2 allowed the electron affinity of Ce and the binding energies of the first two excited states of Ce^- to be calculated. The electron affinity of $\text{Ce}(^1\text{G}_4)$ was determined to be 0.955 ± 0.026 eV. The data also show that Ce^- has at least two bound excited states with binding energies of 0.921 ± 0.025 eV and 0.819 ± 0.027 eV relative to the ($^1\text{G}_4$) ground state of the cerium atom. These bound excited states of Ce^- must be long-lived since the flight time to the interaction region for an ion in the beam was approximately 55 μs . The reported uncertainty in the measurements represents 1 standard deviation of the mean. The uncertainties include statistical and systematic contributions due to the photoelectron count rates for Ce^- and fitting the data to Gaussian functions for the Ce^- , Na^- , and Cu^- photoelectron energy spectra, the uncertainty in the EA of Cu and Na, and the determination of the ion beam energy. The reported uncertainty was dominated by the variance in the energy centroids

resulting from fitting the data to Gaussian function for peaks in the Ce^- photoelectron spectra. This variance was due to the relatively low photoelectron count rates experienced in the Ce^- photoelectron spectra.

In summary, the electron affinity of cerium has been measured using laser photoelectron energy spectroscopy. The electron affinity of $\text{Ce}(^1\text{G}_4)$ was determined to be 0.955 ± 0.026 eV. These results are in disagreement with the EA reported by Berkovits *et al.*, although it is interesting to note that the reported energy separation of the two photodetachment thresholds (2.130 and 2.165 eV) [15] is the same as the energy separation between the ground and first excited states of Ce^- reported here. The present measurements indicate that the electron affinity of cerium is greater than that predicted by O'Malley and Beck [8], who predicted the electron affinity of Ce to be 0.428 eV. Fifteen bound negative ion excited states were also predicted by O'Malley and Beck [8], of which we find evidence for at least two. However, the present experimental sensitivity may be insufficient to determine the existence of more excited, bound states. Strong disagreement between these results and the most sophisticated theoretical calculations available is likely the result of the complexity of Ce^- and the ensuing difficulty in including sufficient electron correlation and relativistic effects in describing the active ($4f$, $5d$, and $6s$) electrons for the cerium atomic anion. In contrast is the LPES experiment mentioned above [16], in which the experimentally determined EA of Lu (which has a closed $4f$ subshell) was found to be in close agreement with a recent theoretical calculation [20].

This work was supported by the National Science Foundation under Cooperative Agreement No. OSR-935227.

[1] T. Andersen, H. K. Haugen, and H. Hotop, *J. Chem. Phys. Ref. Data* **28**, 1511 (1999).

- [2] C. Blondel, *Phys. Scr.* **T58**, 31 (1995).
[3] T. Andersen, *Phys. Scr.* **T34**, 23 (1991).
[4] R. Cowan, *The Theory of Atomic Structure and Spectra* (University of California Press, Berkeley, Los Angeles, 1981).
[5] R. J. Zollweg, *J. Chem. Phys.* **50**, 4251 (1969).
[6] B. M. Angelov, *Chem. Phys. Lett.* **43**, 368 (1976).
[7] S. Bratsch, *Chem. Phys. Lett.* **98**, 113 (1983).
[8] S. M. O'Malley and D. R. Beck, *Phys. Rev. A* **61**, 034501 (2000).
[9] K. Dinov, D. R. Beck, and D. Datta, *Phys. Rev. A* **50**, 1144 (1994).
[10] M. A. Garwan, A. E. Litherland, M.-J. Nadeau, and X.-L. Zhao, *Nucl. Instrum. Methods Phys. Res., Sect. B* **79**, 631 (1993).
[11] M.-J. Nadeau, M. A. Garwan, X.-L. Zhao, and A. E. Litherland, *Nucl. Instrum. Methods Phys. Res., Sect. B* **123**, 521 (1997).
[12] A. M. Covington, D. Calabrese, J. S. Thompson, and T. J. Kvale, *J. Phys. B* **31**, L855 (1998).
[13] M.-J. Nadeau, A. E. Litherland, M. A. Garwan, and X.-L. Zhao, *Nucl. Instrum. Methods Phys. Res., Sect. B* **92**, 265 (1994).
[14] H. H. Andersen, T. Andersen, and U. V. Pedersen, *J. Phys. B* **31**, 2239 (1998).
[15] D. Berkovits, S. Ghelberg, O. Herber, and M. Paul, *Nucl. Instrum. Methods Phys. Res., Sect. B* **123**, 515 (1997).
[16] V. T. Davis and J. S. Thompson, *J. Phys. B* **34**, L433 (2001).
[17] A. M. Covington, D. Calabrese, W. W. Williams, J. S. Thompson, and T. J. Kvale, *Phys. Rev. A* **56**, 4746 (1997).
[18] J. Ho and W. C. Lineberger, *J. Chem. Phys.* **93**, 6987 (1990).
[19] *Atomic Energy Levels—The Rare-Earth Elements*, edited by W. C. Martin, R. Zalubas, and L. Hagan, National Standard Reference Data Series (NSRDS-NBS 60) (National Bureau of Standards, Washington, D.C., 1978), p. 47.
[20] Ephraim Eliav, Uzi Kaldor, and Yasuyuki Ishikawa, *Phys. Rev. A* **52**, 291 (1995).